Stability of heterodyne terahertz receivers

J. W. Kooi[a)]
California Institute of Technology, MS 320-47, Pasadena, California 91125

J. J. A. Baselmans and A. Baryshev
SRON National Institute for Space Research, Sorbonnelaan 2, 3584 CA Utrecht, The Netherlands

R. Schieder
Physikalisches Institute der Universität zu Köln, 50937 Köln, Germany

M. Hajenius and J. R. Gao
SRON National Institute for Space Research, Sorbonnelaan 2, 3584 CA Utrecht, The Netherlands and Kavli Institute of Nanoscience, Delft University of Technology, Lorentzweg 1, 2628 CJ Delft, The Netherlands

T. M. Klapwijk
Kavli Institute of NanoScience, Delft University of Technology, Lorentzweg 1, 2628 CJ Delft, The Netherlands

B. Voronov and G. Gol'tsman
Moscow State Pedagogical University, Moscow 1199992, Russia

(Received 3 November 2005; accepted 19 July 2006; published online 22 September 2006)

In this paper we discuss the stability of heterodyne terahertz receivers based on small volume NbN phonon cooled hot electron bolometers (HEBs). The stability of these receivers can be broken down in two parts: the intrinsic stability of the HEB mixer and the stability of the local oscillator (LO) signal injection scheme. Measurements show that the HEB mixer stability is limited by gain fluctuations with a $1/f$ spectral distribution. In a 60 MHz noise bandwidth this results in an Allan variance stability time of ~0.3 s. Measurement of the spectroscopic Allan variance between two intermediate frequency (IF) channels results in a much longer Allan variance stability time, i.e., 3 s between a 2.5 and a 4.7 GHz channel, and even longer for more closely spaced channels. This implies that the HEB mixer $1/f$ noise is strongly correlated across the IF band and that the correlation gets stronger the closer the IF channels are spaced. In the second part of the paper we discuss atmospheric and mechanical system stability requirements on the LO-mixer cavity path length. We calculate the mixer output noise fluctuations as a result of small perturbations of the LO-mixer standing wave, and find very stringent mechanical and atmospheric tolerance requirements for receivers operating at terahertz frequencies. © *2006 American Institute of Physics*. [DOI: 10.1063/1.2336498]

I. INTRODUCTION

NbN phonon cooled hot electron bolometer (HEB) mixers are currently the most sensitive heterodyne detectors at frequencies above 1.2 THz.[1,2] The present day state-of-the-art mixers combine good sensitivity (8–15 times the quantum limit) with a intermediate frequency (IF) noise bandwidth of 4–6 GHz (Refs. 3–6) up to RF frequencies of at least 5 THz. As a consequence, HEB mixers are increasingly base lined as terahertz heterodyne receivers on astronomical platforms, such as the European space agency's far infrared space observatory (Herschel), the NASA/DLR stratospheric observatory for infrared astronomy (SOFIA), and the Atacama pathfinder experiment (APEX).[8–10] For this reason it is very important to have a good understanding of the time stability of (HEB mixer based) heterodyne terahertz receivers, as this determines the optimal observation strategy.

When an astronomical source is observed, long integrations are generally called for since the signals are deeply embedded in the noise. To extract the weak signals, synchronous detection or Dicke switching[7] (signal–reference) is typically employed to circumvent instabilities in the receiving system. For extended sources this may be accomplished by slewing the entire telescope back and forth, whereas in the case of point sources within the field of view of the telescope, nutating the secondary (or tertiary) mirror is often employed. A practical lower limit for slewing the telescope is generally 15–20 s, while chopping the secondary mirror can perhaps be as fast as 0.2 s (4 Hz). If the noise in the receiver system is completely uncorrelated (white), the subtraction rate (modulation frequency) has no effect on the signal to noise ratio. This can be deduced from the well known radiometer equation[7] which states that white noise integrates down with the square root of the integration time

$$\sigma = \frac{\langle s(t) \rangle}{\sqrt{BT}}. \tag{1}$$

Here $s(t)$ presents the instantaneous output voltage of a spectrometer channel or continuum detector, σ the standard de-

[a)]Electronic mail: kooi@submm.caltech.edu

viation (rms voltage) of the signal, B the effective noise fluctuation bandwidth, and T the integration time of the data set.

In practice the power spectrum of low frequency gain fluctuations and drift noise can be characterized by $S(f) \propto 1/f^{\alpha}$ with $1 \leqslant \alpha < 3$. Typically, $1/f$ (flicker) noise with $\alpha = 1$ originates from electronic devices, though the influence of atmospheric fluctuations in a receiver is often seen to have similar characteristics. Drift noise can be characterized by $2 \leqslant \text{alpha} < 3$, where chaotic processes lead to power laws somewhere in between. White noise, generally of radiometric origin, is described by $\alpha = 0$. A measurement of the Allan variance, defined as $\sigma_A^2 = \frac{1}{2}\sigma_D^2$, is proposed as a powerful tool to discriminate between the various noise terms in the receiver.[11,12] Here σ_D^2 is the variance of the difference of two contiguous measurements of integration time T. It can be shown[11] that for a noise power spectrum $S(f) \propto 1/f^{\alpha}$, the Allan variance is proportional to $T^{\alpha-1}$. For a noise spectrum that contains respectively drift noise, $1/f$ noise, and white noise, the general shape of the Allan variance as a function of integration time is found to be

$$\sigma_A^2(T) = aT^{\beta} + b + c/T, \quad \beta = \alpha - 1, \tag{2}$$

where $1 < \beta < 2$. In practice the last term in the above equation dominates for short integration times and the Allan variance decreases as T^{-1}, as expected for white noise ($\alpha = 0$). For longer integration times, the drift will dominate as shown by the term aT^{β}. In this case, the variance starts to increase with a slope β, which is experimentally found to be between 1 and 2. On certain occasions, such as with the HEB mixers under discussion, it is observed that the variance plateaus. This is denoted by the constant b, and is representative of $1/f$ gain fluctuation (flicker) noise with $\alpha = 1$. Plotting the normalized $\sigma_A^2(t)$ on a log-log plot demonstrates the usefulness of this approach in analyzing the receiver noise statistics. The minimum in the plot, the crossover from white noise to $1/f$ or drift noise, is known as the Allan stability time or Allan minimum time (T_A). Note that T_A is a function of the noise fluctuation bandwidth B according to

$$T_A'/T_A = (B/B')^{1/(\beta+1)}. \tag{3}$$

Hence the Allan time shifts to higher integration times for smaller bandwidths. For the sake of optimum integration efficiency, one is advised to keep the integration time below that of the receiving system. In actual synchronous detection measurements n samples of difference data (signal–reference) are taken, each with a period T. These differences are then averaged so that the total observed time equals $n(2T)$. If the period T is not well below the Allan stability time of the system, then apart from loss in integration efficiency, there will be a problem with base line subtraction. In the averaged output spectrum this will manifest itself as a base line ripple which limits how well the noise integrates down with time. Hence it is of great importance to know the system Allan time and to adjust the measurement strategy accordingly.

In this paper we discuss the stability from two different perspectives. In the first part we consider the fundamental stability of the HEB mixers themselves. We discuss a set of dedicated measurements of the Allan variance on small volume phonon cooled HEB mixers. We start with a measurement of the total power (continuum) Allan variance at 673 GHz. At this frequency there are few uncertainties in the experimental system. Afterwards we measure the total power and the spectroscopic Allan variance at 1.462 THz with an identical HEB mixer at its optimal operating point. In the second part of the paper we discuss the stability of the receiver setup as a whole. We give a theoretical analysis of the mechanical and atmospheric stability issues required to build successful receivers at terahertz frequencies. Due to the much shorter wavelengths, as well as the increasing air loss when compared to, for example, the 650 GHz atmospheric window, the constraints on mechanical design are much more stringent than at submillimeter frequencies. A set of measurements on HEB based receivers between 673 GHz and 2.814 THz with various local oscillator (LO) injection schemes is used to give a solid experimental validation of the theoretical analysis.

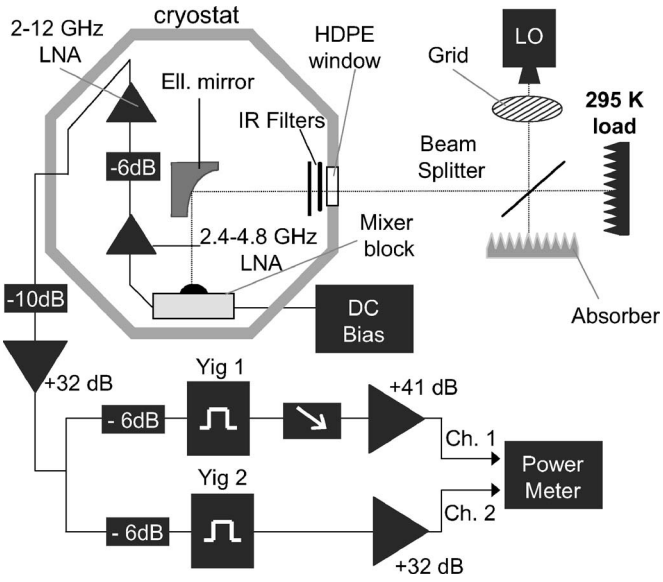

FIG. 1. Schematic picture of the experimental setup.

II. STABILITY OF SMALL VOLUME HEB MIXERS

A. Experimental setup

We describe here in detail the experimental setup used to measure the spectroscopic Allan variance. The device under consideration is a small volume NbN phonon cooled HEB, with a NbN film thickness of about 5 nm, a length of 0.2 μm, and a width of 1.5 μm. The device has a critical current $I_c = 51$ μA at 4.2 K and a normal state resistance of 175 Ω at 11 K. The contact pads between the NbN bridge and the antenna are made by cleaning the NbN layer *in situ* prior to the deposition of 10 nm NbTiN and 40 nm of Au. For details regarding the fabrication we refer to Refs. 3 and 13. To couple the RF radiation to the HEB we use a twin slot antenna[14] designed to give an optimum response at 1.6 THz. In the experiment a quasioptical coupling scheme is used in which the HEB mixer chip is glued to the center of an elliptical silicon lens. A schematic picture of the setup is shown in Fig. 1. The lens is placed in a mixer block with internal

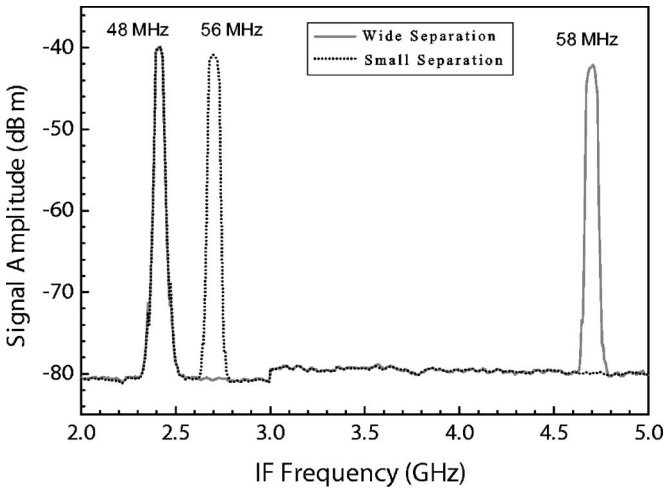

FIG. 2. IF power spectrum of the combination of channels 1 and 2, as shown in Fig. 1. Two measurements are combined in this plot, corresponding to two frequency settings of the YIG filter. In the text the HEB noise properties of closely spaced channels (2.4/2.7 GHz) and widely spaced channels (2.4/4.7 GHz) are studied.

bias Tee and thermally anchored to the 4.2 K plate of an Infrared Laboratories liquid helium cryostat. We use one layer Zitex G104 at 77 K, two layers at 4.2 K as infrared filter, and a 0.9 mm high density polyethylene (HDPE) sheet as vacuum window. A parabolic mirror converts the fast beam from the silicon lens into an $f/D=23.7$ collimated beam with a 3 mm waist located at the cryostat window. The local oscillator consists of a JPL 1.45–1.55 THz multiplier chain,[15] with its input signal provided by a commercial Rhode and Schwarz synthesizer. The chain operates at 1.462 THz where it has a peak output power of 11 μW. A wire grid sets the LO signal attenuation to obtain the desired pumping level for the mixer. The IF output of the mixer unit connects via a 10 cm semirigid Al coax cable to the input of an InP based low noise amplifier (LNA), SRON/Kuo-Liang SN 2, with 2.4–4.8 GHz bandwidth, 25–26 dB of gain, and a noise temperature of 5 K. Because of its low gain this amplifier is connected to a second cryogenic amplifier, a Sandy Weinreb 2–14 GHz SN 20B InP microwave monolythic integrated circuit (MMIC) with 35–36 dB gain and 5 K noise. In between the two amplifiers is a 6 dB attenuator to minimize standing waves. The signal is further amplified at room temperature and is split using a 3 dB power splitter. After the splitter we use in each channel a room temperature GaAs amplifier with a tunable attenuator in one of the channels. A dual frequency power head is then used to measure the power output as a function of time $P(t')$ for two IF channels simultaneously at a rate of 40 times/s. This has been done for IF frequencies very close to each other at the low end of the IF band (2.4 and 2.7 GHz) and for two frequencies near the IF band edges (2.4 and 4.7 GHz). The attenuator equalizes the power in both channels. This is important, since the power meter is a wideband detector with the result that the ratio of in-band signal power to the total power, as seen by the detector, will change the effective measurement bandwidth, and hence the measured Allan variance. In Fig. 2 we give the channel spectral response for both frequency settings. The two channel IF system enables us to do a measurement of the Allan variance in two single IF bins simultaneously. It also enables us to perform a measurement of the spectroscopic (differencing) Allan variance, which is the Allan variance of the difference of two IF channels set to different frequencies.[16] This is the Allan variance of the quantity $s(t')$ given by

$$s(t') = \frac{1}{\sqrt{2}}\left\{\left[\frac{x_i(t')}{\langle x\rangle} - \frac{y_i(t')}{\langle y\rangle}\right] + 1\right\}\frac{\langle x\rangle + \langle y\rangle}{2}, \tag{4}$$

with $x(t')$ and $y(t')$ the original measurements of the powers in each IF channel as a function of time t'. The spectroscopic Allan variance gives the relative stability between channels in an IF band, whereas the total power Allan variance provides the absolute stability per channel bin. Hence it is the spectroscopic Allan variance that is relevant for spectral line measurements. For continuum observations it is the single channel or total power Allan variance that is relevant, with the added difficulty that for continuum observations larger bandwidths are typically used, resulting in a decrease in stability [Eq. (3)].

B. Continuum stability

In the first experiment we measure the bias dependent stability of a small volume HEB mixer, identical to the one described in Sec. II A, at a LO frequency of 673 GHz. We use a similar, but somewhat simpler experimental setup, as described in Sec. II A. A single channel IF system is used, consisting of a mixer block with an external bias Tee, a 1–2 GHz Berkshire GaAs LNA with a 4 K noise temperature, 40 dB gain, followed by a room temperature amplifier (the same as the last amplifier in channel 1 as discussed in Sec. II A and shown in Fig. 2). The IF power is filtered in an 80 MHz bandwidth around 1.45 GHz, and detected with a single channel Agilent power meter at 200 readings/second. The 80 MHz noise bandwidth enables us to omit the additional amplifier after the filter. As LO source we use a phase locked Gunn oscillator with multiplier chain at 673 GHz. The measurements were performed at night in a closed room, and we have taken at least 10 min of data for every measurement. All the data has been used to calculate the Allan variance. The 673 GHz measured double sideband receiver noise temperature (Fig. 3, $T_{N,\mathrm{DSB}}$) is 1100 K, only slightly inferior to the 900 K DSB value at the antenna peak frequency of 1.6 THz. Also indicated in Fig. 3 are all the bias points where we have measured the Allan variance. Results of the measurements are shown in Fig. 4, where panel (a) gives the dependence on LO pump level (i.e., bias current) at the optimal bias voltage, and panel (b) the bias voltage dependence at the optimal LO pump level. Note that the thick line represents, in both plots, the total power Allan time at the optimal operating point. Here T_A is 0.3 s in the 80 MHz noise spectral bandwidth of the setup. A deviation from the radiometer equation by a factor of 2 is already present at $\approx$0.08 s. The plateau in the Allan variance plot indicates that the stability of the NbN HEB mixer suffers from substantial fluctuations in gain, with a $1/f$ power dependence. This is much unlike, for example, SIS mixers where the output noise is primarily dominated by white (−1 slope) and drift noise

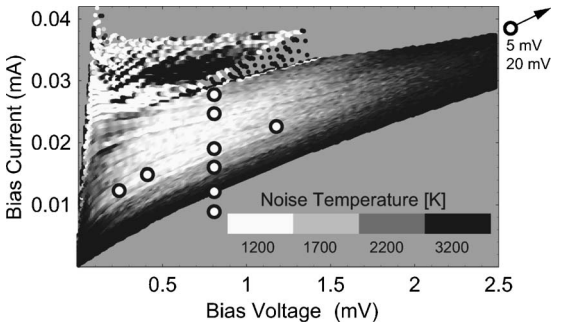

FIG. 3. Noise temperature obtained for all bias points at 673 GHz. We obtain $T_{N,\mathrm{DSB}}=1100$ K, only slightly inferior to the value of $T_{N,\mathrm{DSB}}=900$ K obtained at the antenna center frequency of 1.6 THz. The dots indicate the bias points where the Allan variance has been obtained. The lowest point represents a completely flat pumped *IV* curve, where the mixer has no heterodyne response.

(positive slope).[12] We also observe that T_A increases slowly with increasing dc bias voltage and with increasing LO power (decreasing bias current). However, a noticeable increase in stability is achieved only at bias points ($V>2$ mV or $I\sim 11$ μA) where the receiver sensitivity is already strongly reduced (see Fig. 4). Moreover, we can use the lowest curves in both panels of Fig. 4 to estimate the stability of the experimental setup. The lowest line in Fig. 4(a) is obtained at such a high LO power that the mixer is driven completely normal, i.e., no heterodyne response is observed. The same is true for the line in Fig. 4(b), which is obtained at a high dc bias of 20 mV. In both cases the HEB mixer conversion gain approaches zero, and the HEB behaves as a resistor with a white noise spectrum. As such we would expect a -1 slope in the Allan variance plot. The deviation above ≈ 7 s is due to instabilities in the setup. Being so far away it does not affect the HEB mixer stability measurements we concern ourselves with in this paper. From these results we must conclude that significant gain fluctuations, with a $1/f$-like spectral distribution, limit total power integration times of a small area NbN HEB mixer to about 0.1 s in an 80 MHz noise bandwidth or ≈ 10 ms in a 1 GHz continuum channel. The single channel Allan variance in a typical 1.5 MHz noise spectral bandwidth of an acousto-optical spectrometer[11] is approximately 0.8 s. HEB mixer stability is therefore far inferior to the stability of superconductor-insulator-superconductor (SIS) mixers at the same LO frequency.[12] This has been verified by measuring the stability of a 675 GHz waveguide coupled SIS receiver in the same room using a similar coupling scheme and the same LO source.

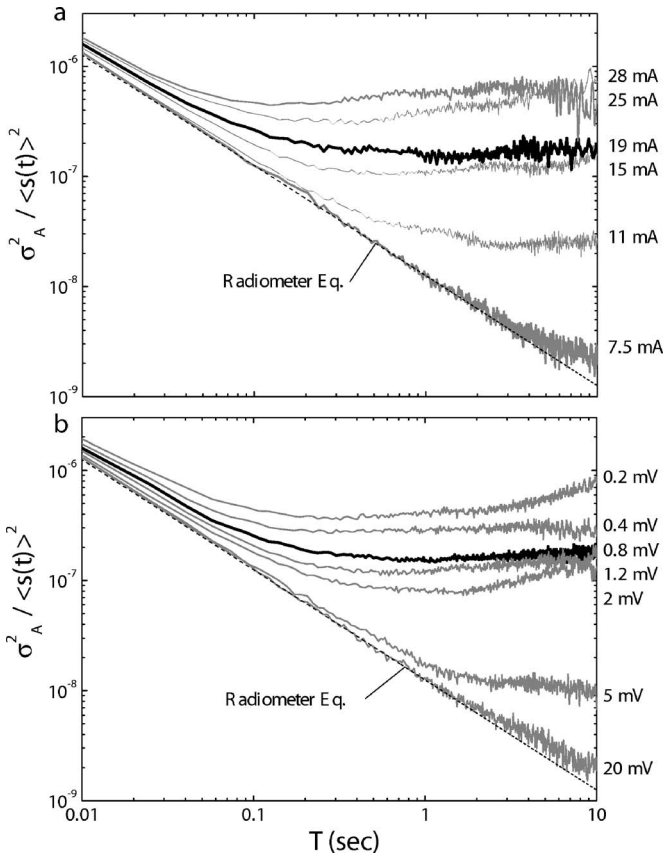

FIG. 4. (a) Normalized total power Allan variance at optimal bias voltage (0.8 mV) for different levels of LO power, as indicated by the resulting mixer bias current. (b) Normalized Allan variance as a function of dc bias voltage at optimal LO power. All bias points are shown as dots in Fig. 3, LO frequency is 673 GHz, and $B\sim 80$ MHz.

C. Spectroscopic stability

In the next experiment we measure the spectroscopic Allan variance, using the exact setup as described in Sec. II A. The HEB mixer used is a different mixer from the one used in the previous experiment; however, it is from the same batch and has an identical normal state resistance, critical current, and sensitivity. The 1.462 THz measurements have again been performed in one single evening in a closed room to minimize disturbances. For every measurement we have taken 48 min of data and we have used the entire data set to calculate the Allan variance. To verify the stability of our setup, and in particular the electrical stability of the amplifiers, yttrium iron garnet (YIG) filters, and the HEB dc bias power supply, we have biased the HEB mixer to 20 mV. The resultant spectroscopic and single channel calibrations are shown by the gray lines in Fig. 5. We observe that the spectroscopic line begins to deviate at ≈ 7 s (~ 50 MHz bandwidth) from the radiometer equation [Eq. (1)], whereas the single channel calibration starts to deviate at about 1 s. This is indicative that some of the drift components in the setup are correlated within the IF band, and that the stability of the setup is therefore slightly worse than in the single channel experiment. This may be related to the fact that the cryogenic amplifiers used in this experiment are InP based. InP devices are known to have more gain fluctuations than their GaAs counterparts. In both situations, however, the stability of the setup is much greater than that of the HEB mixer. Allan variance analysis of the 1.462 THz single channel data shows, once again, that the output noise of a hot electron bolometer suffers from substantial $1/f$ gain fluctuations (0 slope in the Allan variance diagram). The Allan minimum time of 0.4 s is virtually identical to that obtained at optimum bias at 673 GHz (same twin slot device), with a slightly larger filter bandwidth (Fig. 4).

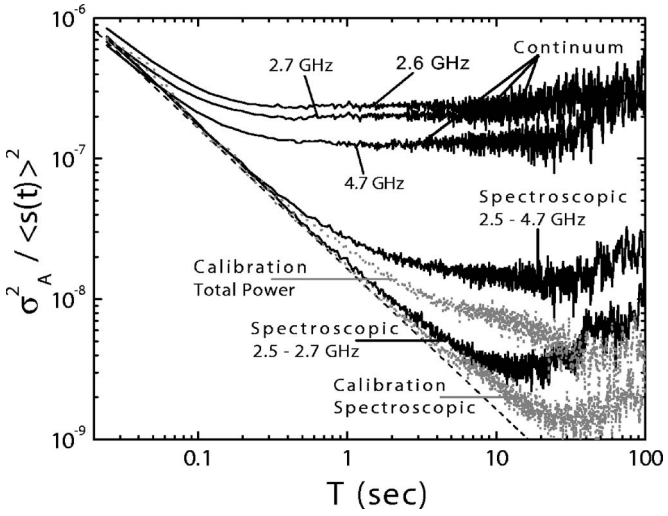

FIG. 5. Normalized spectroscopic and total power Allan variances at 1.462 THz for a small volume twin slot HEB mixer. $B \sim 60$ MHz (refer to Figs. 7 and 8 for details).

The improvement in Allan time by spectroscopic differencing two (or more) channels, as shown in Fig. 5, is seen to be significant (a factor of 10 or better). The spectroscopic Allan variance between 2.4 and 2.7 GHz channels yields an Allan time of 12–13 s. For the 2.4 and 4.7 GHz channels we obtain an Allan time of 2–3 s; however, the deviation from the radiometer equation now occurs at 0.8 s, as opposed to 6 s for the closely spaced channels. In addition, the instability in the widely spaced channels is governed by $1/f$ noise, whereas for the closely spaced channels drift noise is limiting the Allan time. Hence the calculation for the effective integration time in a 1.5 MHz spectral noise bandwidth is a little less straightforward than in the single channel case. Using a $1/f$ spectrum for the widely spaced channels we obtain, in a 1.5 MHz noise bandwidth, a useful integration time of $\sim$80 s. For the 2.4 and 2.7 GHz bins we obtain $\sim$75 s, assuming drift noise with $\beta=1$. Spectroscopic measurements are thus seen to eliminate virtually all $1/f$ mixer noise. Note that the differencing result between 2.4 and 4.7 GHz presents roughly the largest practical bandwidth of a HEB mixer, as the device noise bandwidth is limited to about 4–5 GHz.[3–5] The physical reason for the gain instability is likely related to random processes in the distributed hot-spot mixing region of the bridge, and it is therefore not unreasonable to expect the HEB output noise to be highly correlated. Closely spaced IF channels exhibit a higher degree of correlated noise than the channels that are spaced further apart. The explanation for this phenomena is that the HEB gain bandwidth causes the mixer output noise, dominated by thermal fluctuation noise, to roll off at frequencies above 2–3 GHz. As a result, the HEB output noise at low IF frequencies is dominated by thermal fluctuation noise, whereas at higher IF frequencies the relative Johnson noise contribution increases. For this reason the spectroscopic subtraction is less perfect between IF channels with a large frequency difference. It is also important to note that the traditional way of doing total power Y-factor measurements may not be appropriate for HEB mixers, unless detection methods at time scales less than the single channel Allan time ($<$0.3 s) are employed.

We conclude that the observed $1/f$ gain fluctuations are not only a fundamental property of NbN phonon cooled HEB mixers, but that they are also highly correlated across the IF band. Spectroscopic measurements are therefore very efficient in removing most of the hot electron bolometer output instability, which explains why successful heterodyne spectroscopy observations are possible.[18,19] Continuum observations, such as sky dips or absolute temperature calibration, will, on the other hand, be challenging. It is not inconceivable that device geometry, film properties, and/or magnetic field have an effect on the HEB gain fluctuation noise. As such, small differences in the Allan minimum time may be expected between the different mixer groups. Note that the reported measurements here are in good agreement with other reported stability measurements on similar devices, taking into account variations in (noise) bandwidth.[17]

III. ATMOSPHERIC AND MECHANICAL RECEIVER STABILITY

In the previous section we have focused on the fundamental stability limit of small area HEB based receivers. Up to $\sim$1.46 THz we have seen that the stability of the system is limited by that of the mixer. However, with the development of HEB mixers to frequencies of 5 THz (Refs. 4 and 9) and above, the demands of atmospheric and mechanical stability on the receiving system increase.

In most submillimeter and terahertz receivers the required local oscillator power is coupled to the mixer via optical means, regardless of mixer type. Local oscillator injection is performed most easily via a thin beam splitter, which acts as a directional coupler or diplexer, though it is also possible to use a dual beam interferometer such as a Fabry-Pérot or Martin-Puplett interferometer.[23] Inevitably, due to the finite return loss of the mixer and local oscillator, a standing wave is set up in the LO-mixer cavity. As the LO-mixer cavity path length changes, be it due to air or mechanical fluctuations, the standing wave in the LO-mixer cavity changes amplitude. Amplitude modulation of the local oscillator signal results in short and long term gain instability ($1/f$ noise and drift) at the output of the mixer. Measurements at submillimeter wavelength, with a 10% reflective beam splitter, typically show a LO-mixer standing wave amplitude of 4%–5%. In the terahertz regime, due to shorter wavelength, it is this standing wave that will easily dominate the receiver stability budget. In the next few sections we provide a theoretical analysis of this important effect and compare it to experimental data at 0.673, 1.462, 1.630, and 2.814 THz.

A. LO path length loss

The LO electric field propagating in the z direction can be described as

$$E_{\mathrm{LO}} = E_{\mathrm{LO}}(0)e^{-\gamma z}e^{i\omega t}, \tag{5}$$

with the time averaged power density as

TABLE I. Atmospheric parameters. Air opacity, path length variation ΔL, and air path attenuation for a 1 m column of air. $P_{atm}=990$ mbars, $T=20.15$ °C, and relative humidity of 55%.

Frequency (THz)	0.673	1.462	1.630	2.814
Opacity, τ (Np)	0.01857	0.1238	0.6265	1.0727
ΔL (μm)	62.002	66.202	138.76	140.17
Attenuation (dB)	0.081	0.538	2.72	4.658

$$P_{LO} = P_{LO}(0)e^{-\tau z}. \tag{6}$$

γ is known as the complex propagation constant, τ the opacity/meter, and $P_{LO}(0)$ the peak LO power at $z=0$ m. The air opacity and the change in optical path length ΔL, defined as the path length increase due to water vapor in a 1 m column of air, have been modeled by Pardo *et al.*[20,21] and provided in Table I. Uncertainty in the opacity is estimated to be no more than 5%. The conditions used are as follows: atmospheric pressure of 990 mbars, temperature of 20.15 °C, and relative humidity of 55%. Note that in the case of turbulent air, it is not the absolute path length we concern ourselves with, but the deviation in path length due to changes in the refractive index of air.

B. Standing waves in the LO-mixer path

Following Schieder[22] and Goldsmith,[23] we define the incident LO power on the mixer, P_{LO}, as

$$P_{LO} = P_{LO}(0)|r_{BS}|^2 A_i(\nu_{LO}). \tag{7}$$

$|r_{BS}|^2$ is the beam splitter or diplexer power reflection coefficient, $P_{LO}(0)$ the LO power at the LO source output, and $A_i(\nu_{LO})$ the Airy function that describes the fractional transmitted power as a function of the LO-mixer distance z.

$$A_i(\nu_{LO}) = \frac{1}{1 + F\sin^2(\delta/2)}, \quad \delta = \frac{4\pi n z}{\lambda}, \tag{8}$$

where n is the refractive index of air, given by $n=(1+\Delta L/z)$ and F the finesse of the LO-mixer cavity,

$$F = \frac{4|r|^2}{(1-|r|^2)^2}. \tag{9}$$

Here $|r|^2$ represents internal reflections in the LO-mixer cavity. Rewriting Eq. (9) to include loss, we substitute $|r|^2 \rightarrow |r|^2 e^{-\tau z}$ so that

$$F = \frac{4|r|^2 e^{-\tau z}}{(1-|r|^2 e^{-\tau z})^2}. \tag{10}$$

Now substituting Eq. (10) into Eq. (8), and expressing the Airy function in terms of the propagation constant β gives

$$A_i(\nu_{LO}) = \frac{(1-|r|^2 e^{-\tau z})^2}{(1-|r|^2 e^{-\tau z})^2 + 4|r|^2 e^{-\tau z}\sin^2(\beta n z)}, \tag{11}$$

where $|r|^2$ can be expressed in terms of the mixer reflection coefficient $|r_m|^2$, the LO source reflection coefficient $|r_{LO}|^2$, and the beam splitter or diplexer reflection coefficient $|r_{BS}|^2$ according to

$$|r|^2 = |r_{BS}|^2\sqrt{|r_m^2 r_{LO}^2|}. \tag{12}$$

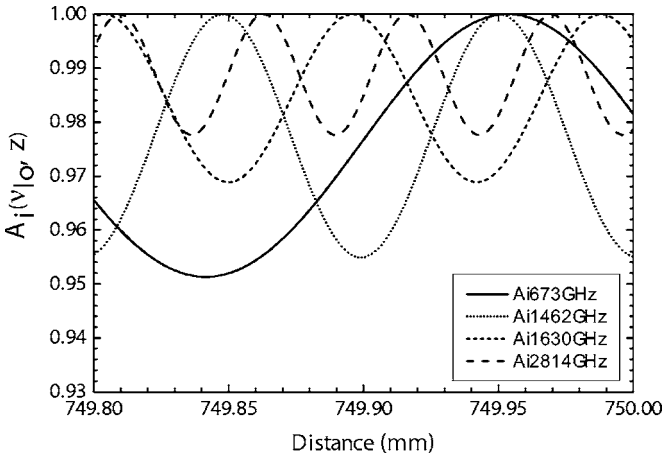

FIG. 6. Standing wave for a cavity path length of $z=0.75$ m. Note the effect of atmospheric loss (damping) on the standing wave amplitude at the shorter wavelength. Shown here are the last 200 μm. In the example $|r_m|^2$ was taken to be −10 dB, $|r_{LO}|^2=-8$ dB, and $|r_{BS}|^2=-10$ dB. Without atmospheric loss (space or a high dry mountain site), the peak-to-peak standing wave amplitude in the example would be 4.934%.

Looking at Eq. (11), we see that the Airy function has a ripple period of $\beta n z=\pi$. This describes the standing wave pattern between the LO port and the mixer input via the beam splitter. In the next sections we examine the importance of tuning to the peak of the LO-mixer cavity standing wave ($\beta n z=0,\pi,2\pi,\ldots$), rather than on a steep slope ($\beta n z=\pi/4,3\pi/4,\ldots$).

Consider, as an example, a typical mixer with an input reflection coefficient of −10 dB ($|r_m|^2=0.10$), a LO source reflection coefficient of −8 dB ($|r_{LO}|^2=0.16$), and a 10% (−10 dB) beam splitter to inject the local oscillator signal. In Fig. 6 we plot the Airy function [Eq. (11)] for the last 200 μm of a $z=0.75$ m LO-mixer cavity path length. If there were no atmospheric loss (space or vacuum cryostat), the peak-to-peak amplitude variation for the given parameters would be 4.934%. In actuality, for a 0.75 m path length, the standing wave amplitude has attenuated to ≈4.8% for a 673 GHz local oscillator signal, 3.1% for the 1.630 THz CH_2F_2 FIR laser line, and 2.2% for the quantum cascade laser (QCL) line at 2.814 GHz (Ref. 24) (close to the 2.774 THz water line). Interestingly, a 5% standing wave value agrees well with measurements at 230, 352, 690, and 807 GHz obtained at the Caltech Submillimeter Observatory (CSO), a nice confirmation that the assumed mixer, LO source, and beam splitter reflections are reasonable. From Eq. (11) it is clear that as $r_{BS}\rightarrow 0$ the LO-mixer standing wave amplitude also vanishes to zero. It is advantageous therefore to use a LO diplexing scheme with a small coupling coefficient. Of course, at terahertz frequencies, except when a FIR laser is employed, this may not be practical due to the limited available LO power.

C. Estimate of allowed LO power fluctuations

To estimate the level of local oscillator fluctuations that may be tolerated without degrading the receiver stability below that of the mixer stability, one has to consider the sensitivity of the mixer IF output power with respect to the input

LO power (dP_{IF}/dP_{LO}). Assuming that the mixer acts as a standard square law detector, the IF output will be proportional to changes in the input signal. For this reason, tiny LO fluctuations (amplitude noise) at the mixer input show up as instability at the mixer IF output. Since atmospheric and mechanical vibrations typically have a $1/f$ spectral distribution, care should be taken to keep these fluctuations on time scales longer than the intrinsic stability time of the HEB mixer. From the total power stability measurements (see Figs. 7 and 8) and using Eq. (1) with $T=T_A$, we find that local oscillator changes at the mixer $[\sigma/\langle s(t)\rangle]$ in excess of 0.025% result in output fluctuations larger than the (small volume) HEB mixer $1/f$ noise. In this case the local oscillator signal fluctuations begin to dominate the HEB mixer total power stability budget.

D. Sensitivity to atmospheric turbulence

To estimate the level of local oscillator fluctuations in the presence of turbulent air, we calculate the change in LO power [Eq. (11)] against the percentage change in optical path length ΔL (Fig. 7). If the air were to be absolutely stable, or humidity very low, as would be the case on a high mountain, we would expect $dP_{LO} \rightarrow$ zero. Note that the loss term in Eq. (11) has a damping effect on the LO standing wave amplitude. For instance, if a mixer is to be operated close to a water line, fluctuations in the refractive index of air will be significant and will modulate the standing wave amplitude. This is, however, somewhat mitigated by the increased absorption in air. The increase in sensitivity to air turbulence with frequency is therefore not only a function of wavelength, but also of atmospheric opacity.

In Fig. 7 we plot the result of this calculation for four frequencies, evaluated for a LO-mixer path length of $z=0.75$ m, and a 10% reflecting beam splitter. When the LO-mixer standing wave is tuned to a peak ($\beta nz=0,\pi,2\pi,\ldots$), the effect of air turbulence on the local oscillator signal at the mixer is smallest. In this situation, assuming a maximum LO signal fluctuation of 0.025% (Sec. III C), the allowed atmospheric path length change due to air turbulence at 1.462 THz is ±4.8%. At the 1.630 THz CH_2F_2 far infrared (FIR) laser line this is ±2.4%, and at the 2.814 THz quantum cascade laser line[24] it has become a mere ±1.3%. At 650 GHz the atmosphere has essentially no influence on the local oscillator signal, as is observed in practice. Reducing the path length and/or atmospheric humidity (high mountain) will considerably improve the situation. However, when a dual beam interferometer type of LO injection scheme is employed,[23] the allowed optical path length change decreases by approximately a factor of 3. This assumes a 1 dB loss in the optics setup.

If we tune the local oscillator frequency to the most sensitive part of the standing wave ($\beta nz=\pi/4,3\pi/4,\ldots$), we see a large increase in LO power fluctuation for a given change in optical path length. It is absolutely critical therefore, as far as terahertz receiver stability is concerned, that the LO-mixer cavity is tuned to a peak of the LO power standing wave. In practice this may be done by adjusting the LO frequency or by a small positional move of the cryostat along the axis of propagation.

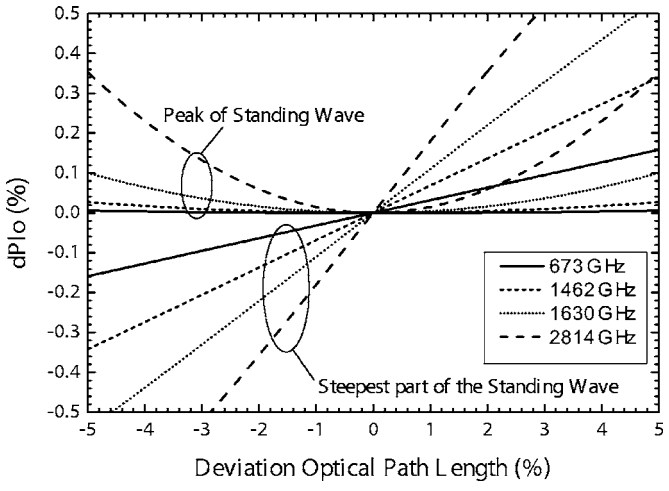

FIG. 7. Change in LO power as function of change in optical path length for a $z=0.75$ m cavity. $|r_m|^2$ is −10 dB, $|r_{LO}|^2$ −8 dB, and $|r_{BS}|^2$ −10 dB. Shown is a situation where the cavity length is tuned to the peak of the LO-mixer standing wave ($\beta nz=0,\pi,2\pi,\ldots$) and where dP_{LO}/dz has a maximum. For a 0.025% change in LO power (Sec. III B), the maximum allowed change in optical path length is just a few percent. The situation degrades by approximately a factor of 3 in the case of a dual beam interferometer style LO diplexing scheme.

E. Sensitivity to mechanical fluctuations

As an example of the effect of mechanical path length fluctuations, consider the same mixer with an input reflection coefficient of −10 dB, LO source reflection coefficient of −8 dB, and a 10% reflecting beam splitter to inject the LO signal. Evaluating Eq. (11) for small perturbations in z, we obtain an estimate for the allowed mechanical path length change of the LO-mixer cavity. Given again a 0.025% local oscillator signal stability (Sec. III C), the mechanical stability of the instrument at 1.462 THz needs to be better than ±2.4 μm, ±2.6 μm at 1.630 THz, and a mere ±1.8 μm at 2.814 THz. As seen in the previous section, if a dual beam

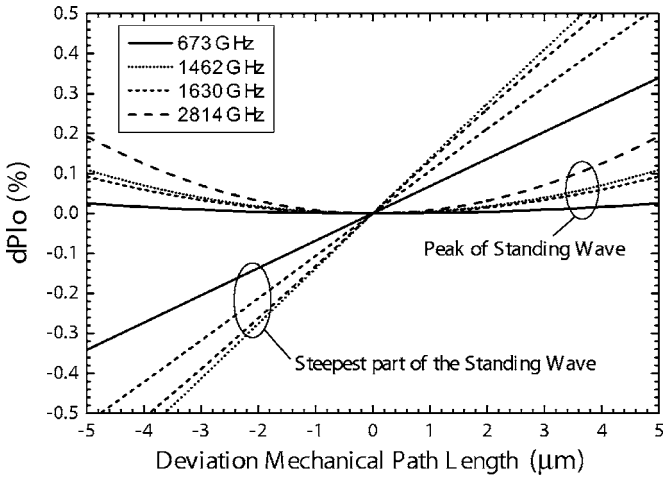

FIG. 8. Change in LO power as a function of change in mechanical path length for a $z=0.75$ m cavity. $|r_m|^2$ equals −10 dB, $|r_{LO}|^2$ −8 dB, and $|r_{BS}|^2$ −10 dB. Data is given when the cavity length is tuned to a peak of the standing wave and on the steepest slope where $\beta nz=\pi/2,3\pi/2,\ldots$. When dP_{LO}/dz has a maximum the mechanical stability requirements become considerably more stringent.

interferometer style diplexer is employed the sensitivity to mechanical change increases approximately threefold. In this case mechanical stability on the order of 0.75 μm (or less) is called for. This specification places stringent thermal requirements on the hardware. For example, given a thermal expansion of aluminum at room temperature of 2.25×10^{-5} K^{-1}, a 75 cm LO-mixer cavity path length, and a total integration/calibration period of 20 min, the maximum allowed temperature drift will be ~132 mK/h. At a physical temperature of 100 K the situation improves by approximately a factor of 2 due to a decrease in the thermal expansion of aluminum. These numbers suggest that in the terahertz regime LO injection is best accomplished in a temperature controlled environment or at cryogenic temperatures where thermal fluctuations are minimized. Furthermore, the analysis suggests that if the LO-mixer cavity length is fixed (LO source and receiver cannot be moved), observations should be done at discrete frequencies such that βnz is a multiple of π radians. This is the free spectral range, which for $z=75$ cm equals 200 MHz.

IV. EXPERIMENTAL VALIDATION

To experimentally study the effect of the atmosphere and mechanics at higher frequencies, we have repeated the stability measurement using a QCL as the local oscillator source.[24] As mixer a spiral antenna coupled, large volume (0.4×4 μm) hot electron bolometer was used. We show in Fig. 9 the measured Allan variance at 2.814 THz, using the QCL as LO source[24] with a 6 μm Mylar beam splitter. The measured Allan variance at 1.5228 THz was obtained with a solid state LO source similar to the one used in the experiments described in Sec. II. The LO is coupled directly to the mixer in this case. Superimposed on the plots are also the results from Fig. 8. Note that the Allan variance time is roughly identical for all data sets, being governed by intrinsic HEB $1/f$ gain fluctuation noise. However, at 2.8 THz we see the combined effect of atmospheric and mechanical drifts. The same is true, to a lesser extent, for the 1.5228 THz data. The clear presence of drift in the 1.5228 THz data contrasts the absence of drift at 1.4624 THz, despite the fact that atmospheric properties and mechanical tolerances are very similar for both frequencies. The explanation for this is that in the 1.462 THz measurement a 3.5 μm beam splitter had been used, whereas in the 1.5228 THz experiment the local oscillator signal was coupled directly to the mixer. The much stronger drift component at 1.5228 THz is consistent with the developed theory, and provides an indication of what may happen if a room temperature dual beam interferometer style diplexer is used to inject the local oscillator signal. Because the HEB output noise is so dominated by internal $1/f$ gain fluctuations, the discussed atmospheric and mechanical stability issues in the case of HEB mixers is somewhat muted below 2 THz, unlike, for example, in the case of SIS or Schottky based receivers.

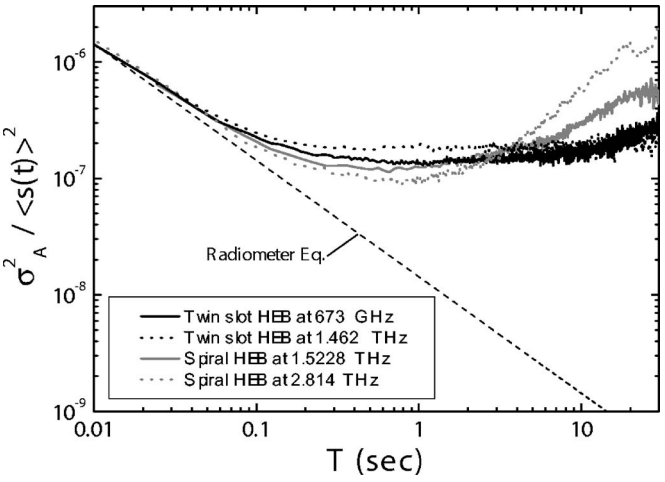

FIG. 9. Normalized total power Allan variance stability measurements for a variety of local oscillator sources, devices, and LO frequencies. In all cases the HEB output noise exhibits an Allan minimum time of 0.2–0.3 s. For the 1.4624 THz and 673 GHz data the HEB output noise at the longer integration times is entirely dominated by gain fluctuation noise with a $1/f$ spectral distribution. At 1.5228 and 2.814 THz atmospheric and mechanical drifts become progressively worse. Note that at 1.5228 THz the LO signal was injected directly, whereas in all other experiments a very thin beam splitter was employed ($|r_{BS}|=-12$ dB at 2.814 THz and -15 dB for all other frequencies).

V. CONCLUSION

We have studied the stability of HEB heterodyne receivers from two perspectives. First we have measured the stability of a HEB mixer in a laboratory setup at 0.673, 1.462, 1.630, and 2.814 THz. We find that phonon cooled NbN HEB's have significant short term gain fluctuation noise, and that up to at least 2.8 THz $1/f$ noise dominates the mixer stability budget. This instability limits the useful integration time to about 0.3 s in an 80 MHz total power noise fluctuation bandwidth. The physical origin of the gain fluctuation noise is unclear; however, it is conjectured that it may be related to thermal or quantum processes in the hot-spot region of the mixer. It is therefore advisable to establish sensitivity of terahertz HEB mixers via synchronous or spectroscopic means, keeping integration times below the intrinsic Allan variance stability time of the mixer.

The level of improvement that may be gained from using the spectroscopic measurement (statistically differencing two or more uncorrelated IF channels) depends on how correlated the noise is across the HEB IF band. Depending on the IF bandwidth under consideration, we have observed a factor of 10–15 improvement in stability with a small area of 0.15×1.0 μm phonon cooled HEB. This is significant, as it demonstrates that the $1/f$ output noise of the HEB mixer is highly correlated, and why therefore hot electron bolometers may still be used as effective heterodyne mixing elements. It should be noted that if science goals call for the hot electron bolometer mixer to be used in continuum observations, spectroscopic stability measurements are not a good guide for performance. Whichever stability method is relevant (continuum or spectroscopic) will thus depend on the science objectives of the instrument.

Finally, we have studied the effect of atmosphere, mechanics, and temperature on the stability on terahertz mixers from the point of view of the LO-mixer cavity standing wave. It is found that operating terahertz receivers at the peak of the LO-mixer standing wave is important. Due to the

very stringent thermal requirements, a dual beam interferometer style LO injection scheme is found to be best employed cold, i.e., at cryogenic temperatures. There are, of course, other mechanisms that cause a mixer to behave unstably or erratically.[11,12] Fortunately, spectroscopic measurements greatly reduce many of these problems as fluctuations are often highly correlated. However, if the spectroscopic Allan stability time of the instrument is found to be less than 20 s, the typical position switching time of a telescope, observations of extended astronomical sources may become problematic.

ACKNOWLEDGMENTS

We wish to acknowledge Serguei Cherednichenko and Therese Berg for very helpful HEB performance discussions, Juan Pardo for his help in modeling atmospheric conditions encountered in the laboratory, and Wolfgang Wild for his unwavering support and coordination. This work was supported in part by NSF Grant No. AST-0229008 and Radionet.

[1]E. M. Gershenzon, G. N. Goltsman, I. G. Gogidze, A. I. Eliantev, B. S. Karasik, and A. D. Semenov, Sov. Phys. Supercondcutivity **3**, 1582 (1990).
[2]D. E. Prober, Appl. Phys. Lett. **62**, 2119 (1993).
[3]J. J. A. Baselmans, J. M. Hajenius, J. R. Gao, T. M. Klapwijk, P. A. J. de Korte, B. Voronov, and G. Gol'tsman, Appl. Phys. Lett. **84**, 1958 (2004).
[4]A. D. Semenov, H.-W. Hübers, J. Schubert, G. N. Gol'tsman, A. I. Elantiev, B. M. Voronov, and E. M. Gershenzon, J. Appl. Phys. **88**, 6758 (2000).
[5]S. Cherednichenko, P. Khosropanah, E. Kollberg, M. Kroug, and H. Merkel, Physica C **407**, 372 (2002).
[6]P. Yagoubov, M. Kroug, H. Merkel, E. Kollberg, G. Gol'tsman, S. Svechnikov, and E. Gershenzon, Appl. Phys. Lett. **73**, 2814 (1998).
[7]J. D. Kraus, *Radio Astronomy* (McGraw-Hill, New York, 1966), Chaps. 3 and 7.
[8]Herschel (http://sci.esa.int/).
[9]SOFIA (http://www.sofia.usra.edu/).
[10]APEX (http://www.apex-telescope.org/).
[11]R. Schieder and C. Kramer, Astron. Astrophys. **373**, 746 (2001).
[12]J. W. Kooi, G. Chattopadhyay, M. Thielman, T. G. Phillips, and R. Schieder, Int. J. Infrared Millim. Waves **21**, 689 (2000).
[13]M. Hajenius, J. J. A. Baselmans, J. R. Gao, T. M. Klapwijk, P. A. J. de Korte, B. Voronov, and G. Goltsman, Supercond. Sci. Technol. **17**, S224 (2004).
[14]W. F. M. Ganzevles, L. R. Swart, J. R. Gao, P. A. J. de Korte, and T. M. Klapwijk, Appl. Phys. Lett. **76**, 3304 (2000).
[15]G. Chattopadhyay, E. Schlecht, J. Ward, J. Gill, H. Javadi, F. Maiwald, and I. Mehdi, IEEE Trans. Microwave Theory Tech. **52**, 51538 (2004).
[16]V. Tolls, R. Schieder, and G. Winnewisser, Exp. Astron. **1**, 101 (1989).
[17]T. Berg, S. Cherednichenko, V. Drakinskiy, H. Merkel, E. Kollberg, and J. W. Kooi, Proceedings of the 15th International Symposium on Space Terahertz Technology, Northampton, Massachusetts, 2004 (unpublished).
[18]J. Kawamura *et al.*, Astron. Astrophys. **394**, 271 (2002).
[19]M. C. Wiedner *et al.*, Astron. Astrophys. **454**, L33 (2006).
[20]J. R. Pardo, E. Serabyn, M. C. Wiedner, and J. Cernicharo, J. Quant. Spectrosc. Radiat. Transf. **96**, 537 (2005).
[21]J. R. Pardo, J. Cernicharo, and E. Serabyn, IEEE Trans. Antennas Propag. **49**, 1683 (2001).
[22]R. Schieder (private communication).
[23]P. F. Goldsmith, *Quasioptical Systems* (IEEE, New York, 1998), Chap. 9.
[24]J. R. Gao *et al.*, Appl. Phys. Lett. **86**, 244104 (2005).